Nanoscale

CrossMark
← click for updates

Catalytic effect of ultrananocrystalline Fe₃O₄ on algal bio-crude production *via* HTL process†

Arnulfo Rojas-Pérez,[a] Daysi Diaz-Diestra,[a,b] Cecilia B. Frias-Flores,[a]
Juan Beltran-Huarac,[a,b] K. C. Das,[c] Brad R. Weiner,[a,b] Gerardo Morell[a,b] and
Liz M. Díaz-Vázquez*[a]

We report a comprehensive quantitative study of the production of refined bio-crudes *via* a controlled hydrothermal liquefaction (HTL) process using *Ulva fasciata* macroalgae (UFMA) as biomass and ultrananocrystalline Fe₃O₄ (UNCFO) as catalyst. X-ray diffraction and electron microscopy were applied to elucidate the formation of the high-quality nanocatalysts. Gas chromatography-mass spectroscopy (GC-MS) and CHNS analyses showed that the bio-crude yield and carbon/oxygen ratios increase as the amount of UNCFO increases, reaching a peak value of 32% at 1.25 wt% (a 9% increase when compared to the catalyst-free yield). The bio-crude is mainly composed of fatty acids, alcohols, ketones, phenol and benzene derivatives, and hydrocarbons. Their relative abundance changes as a function of catalyst concentration. FTIR spectroscopy and vibrating sample magnetometry revealed that the as-produced bio-crudes are free of iron species, which accumulate in the generated bio-chars. Our findings also indicate that the energy recovery values *via* the HTL process are sensitive to the catalyst loading, with a threshold loading of 1.25 wt%. GC-MS studies show that the UNCFO not only influences the chemical nature of the resulting bio-crudes and bio-chars, but also the amount of fixed carbons in the solid residues. The detailed molecular characterization of the bio-crudes and bio-chars catalyzed by UNCFO represents the first systematic study reported using UFMA. This study brings forth new avenues to advance the highly-pure bio-crude production employing active, heterogeneous catalyst materials that are recoverable and recyclable for continuous thermochemical reactions.

Introduction

Hydrothermal liquefaction (HTL) is a feasible alternative for the conversion of wet biomass into biofuels. This process involves direct liquefaction using water as both a reactive medium and a catalyst to convert biomass into liquid crude under controlled environments.[1] At sub-critical conditions, HTL converts biomass into oil rather than gases due to its superior ionic product (K_w) and lower dielectric constant, when compared to those found at standard conditions.[2] Such conversion consists of the breakdown of the main constituents (such as polysaccharides, lipids and proteins) into simpler molecules, which are recombined to form a series of hydrocarbons with high caloric values.[3] After hydrothermal oxidation, the heteroatoms present in the biomass produce valued byproducts, including liquid bio-crude, solid residues, and aqueous and gaseous fractions, which can be separated and characterized. Thus, the HTL process enables an increase in the crude yield from the biomass by controlling the experimental conditions inside the HTL reactor, such as temperature (280–370 °C), pressure (10–25 MPa), solvent and catalyst concentrations, and feedstock compositions.[4,5] This fast, eco-friendly, and energetically efficient process now represents a promising alternative to fossil fuels.

Recently, the production of bio-crude employing macroalgae as a potential biomass source has been considered due to their high energy content, low life-cycle emission of greenhouse gases, relatively fast growth rates, ease of harvesting and cost-effectiveness.[6] For instance, they possess higher lipid contents than most lignocellulosic biomass (such as plants and wood) used for biofuels, and are primarily composed of alginic acid, laminarin, carrageenan and agarose, which are critical to facilitate thermochemical conversion processes.[7] Although the HTL process has the potential to generate high yields of bio-crude, there are some limitations to using macroalgae biomass as a feedstock. In addition, macroalgae exhibit high ash content (up to 50%) due to the presence of inorganic salts and metals, which restricts their use in direct combustion and

[a]Department of Environmental Sciences, Physics and Chemistry, University of Puerto Rico, San Juan, PR 00936, USA. E-mail: lizvazquez8@gmail.com
[b]Molecular Science Research Building, University of Puerto Rico, San Juan, PR 00926, USA
[c]Biorefining and Carbon Cycling Program, Department of Biological and Agricultural Engineering, University of Georgia, Athens, GA 30602, USA
†Electronic supplementary information (ESI) available. See DOI: 10.1039/c5nr04404a

gasification processes. Few studies have reported the effect of ash content in HTL conversion of marine feedstock (such as macroalgae).[8] The high inorganic content in macroalgae would affect the physicochemical characteristics of the bio-crude and its storage through the catalysis of polymerization reactions. Neveux et al.[3] compared the bio-crude yield of six macroalgae using a stainless steel reactor covering a temperature range of 330–341 °C and pressures between 140–170 bar, finding that *Ulva ohnoi* exhibits a high crude yield of ~18.7 wt%. Singh et al.[4] evaluated the use of ethanol, methanol and water as solvents in the liquefaction of *Ulva fasciata*. The total crude yield obtained was 11 wt% for water, 40 wt% for ethanol, and 44 wt% for methanol, showing that alcohols increase the bio-crude yield acting not only as co-solvents but also as hydrogen donors that promote further transesterification reactions.

More recently, efforts have been devoted to investigating the effect of catalysts on the HTL process and its correlated efficient path to produce high-quality bio-crude.[5,9] Among the most used catalysts, solid nanocatalysts have drawn special attention due to their high chemical and physical stability and larger chemically-active surface areas, both being critical factors in industrial applications.[10,11] Nonetheless, the recovery of the solid catalysts from the bio-crude mixture *via* conventional filtration process is generally not cost-effective. For this reason, it is important to develop heterogeneous catalyst materials that are recoverable and recyclable for continuous thermochemical reactions. In this context, iron oxide-based nanocatalysts have been proposed as an alternative because they can be effectively separated by means of magnetic fields,[12] thus enhancing their lifetime and cost-effectiveness. Moreover, iron oxide nanostructures possess large specific surfaces, low mass transfer resistance, and improved catalytic activity for photocatalysis, biocatalysis, and phase-transfer catalysis.[13] Few studies on the bio-diesel production using iron oxide-based nanocatalysts through transesterification have been reported to date. Ying et al.[14] used a magnetic cell biocatalyst immobilized in hydrophobic magnetic polymicrosphere for the transesterification of waste cooking oils with methanol, obtaining a conversion up to 90%. Xie et al.[15] immobilized lipase on Fe_3O_4 nanoparticles (NPs) as a catalyst for biodiesel production by transesterification of soybean oil with assisted-methanol, and achieved a conversion over 90%. Hu et al.[16] prepared a magnetic porous nanocatalyst based on $KF/CaO–Fe_3O_4$ and obtained a fatty acid methyl esters yield of 95%. Hence, iron oxide-based nanocatalysts exhibit high catalytic activity and significant advantages for easy magnetic separation and reusability. However, this research field is still at its infancy and further investigation on the bio-crude yield is needed. Furthermore, the bio-crude production *via* HTL assisted by Fe_3O_4 catalysts using marine products as feedstock remains a big challenge.

In this study, we report for the first time the quantitative effect of ultrananocrystalline Fe_3O_4 (UNCFO) catalyst on the production of refined bio-crude *via* a controlled HTL process using *Ulva fasciata* macroalgae (UFMA) as biomass. A compre-hensive analysis of the molecular characterization of the bio-crudes is presented. The ability of the UNCFO catalyst to influence the chemical composition of the resulting bio-crudes and the amount of fixed carbon in the solid residues is also discussed.

Experimental techniques

Materials

All reagents used in this investigation, iron(II) chloride tetrahydrate ($FeCl_2 \cdot 4H_2O$), iron(III) chloride hexahydrate ($FeCl_3 \cdot 6H_2O$), dichloromethane (CH_2Cl_2) and sodium hydroxide (NaOH), were analytical-grade (>99.999%) and purchased from Sigma Aldrich, USA, and were used directly without any further processing.

Fabrication of UNCFO

The catalyst was synthesized *via* the co-precipitation method[17] with minor modifications. Briefly, $FeCl_2 \cdot 4H_2O$ and $FeCl_3 \cdot 6H_2O$ were dissolved into high-purity deionized water with a molar ratio of 2:1, respectively. An aqueous solution of NaOH (0.440 M) was added and quickly subject to vigorous mechanical stirring (4000 rpm) at 100 °C for 30 min, keeping the volume constant and at an adjusted pH. The solution was then magnetically decanted, abundantly washed and dried under a controlled environment for 24 h.

Characterization of UNCFO

The crystalline structure of the products was studied using an X-ray diffractometer (XRD), Model Siemens D5000 with Cu K_α radiation. The surface morphology and size were analyzed using a JEOL JEM-2200FS Cs-corrected high-resolution transmission electron microscope (HRTEM). All the images were taken in scanning TEM (STEM) mode. The magnetic properties were measured with a vibrating sample magnetometer (VSM, Lakeshore 7400).

Macroalgae biomass

UFMA biomass was collected in August 2014 at Fajardo, Puerto Rico (18.3258° N, 65.6525° W), located on the east coast of the island facing the Atlantic Ocean. Impurities and salts were removed using distilled water. Macroalgae biomass was dried, pulverized and stored in a desiccator at room temperature until further analysis. Biomass was first analyzed in order to identify its content in soluble carbohydrates, total proteins and lipids. Anthrone's method[18] was followed to determine the total soluble carbohydrates content using an UV-Vis spectrophotometer (Hach Dr5000). The protein content in algal biomass was ascertained by bicinchoninic acid assay.[19] The total lipid content (%) was determined using the Bligh and Dyer's method with minor adaptations.[20] Briefly, 1 g of the biomass was homogenized using 15.0 mL of a mixture of solvents (chloroform/(methanol/water) 3:1). The homogenate was transferred to a separation funnel, and then chloroform (15 mL) was added. The aqueous phase was discarded and the

organic extract was collected and evaporated until dry in weighed vials to determine the total lipid content of the products. Moisture and Ash content were calculated in triplicate measurements for 10 mg of UFMA using a thermogravimetric analyzer (Perkin Elmer TGA 4000). The TGA analysis conditions were the following: oxygen flow rate of 20 mL min^{-1}, heating rate of 20 °C min^{-1} from 24 to 800 °C and holding time of 30 min.

HTL methodology

HTL experiments were carried out in a 350 mL batch reactor system (Parr Instruments Co. Moline, PA, USA) at the optimal reaction conditions reported by Singh *et al.*[4] for the same biomass (300 °C, 15 min, 100 rpm). In a typical experiment, 13 wt% of dry algae in distilled water, were loaded into the HTL reactor with different UNCFO loadings (0, 0.63, 1.25, 2.50 and 3.75 wt%). The system was purged with He for 3 min and pressurized to 60 psi. At the end of the reaction, the reactor was cooled spontaneously to room temperature. The gas phase was vented and the remaining products were separated in bio-crude and water-soluble fractions and solid residues as reported in our previous work. Briefly[8] the liquid phase was filtered using vacuum filtration to remove the solid residues. These residues were washed with DCM to extract all of the bio-crude in the sample. A liquid–liquid extraction was carried out to separate the DCM phase from the aqueous phase. Afterwards, the DCM phase was rotovaporated in order to obtain the concentrated bio-crude product.

Bio-crude and bio-char analysis

Bio-crude and bio-char were analyzed using a FTIR-ATR spectrometer (Perkin Elmer Spectrum 100 FTIR). The content of elemental C, H, N, S, and O in the bio-crude and bio-char was measured using a LECO brand analyzer (Model CHNS-932). Gas chromatography and mass spectroscopy (GC-MS) analyses of the bio-crude were carried out with an Agilent Technologies 6890N Network GC system, 5973 Network Mass selective Detector and Agilent JW Scientific GC column (Biodiesel EN14103). A detailed GC-MS procedure can be found in ref. 8. Bio-crude and bio-char product yields were calculated separately on an ash and moisture-free weight basis using the following equation:[21]

$$Y_{PRODUCT} = \left[\frac{W_{PRODUCT}}{(W_{FEEDSTOCK} - W_{ASH} - W_{MOISTURE})} \right] \times 100 \quad (1)$$

where $Y_{PRODUCT}$ is the bio-crude or bio-char yield (wt%) on a dry weight basis. $W_{PRODUCT}$ is the mass of product (g). $W_{FEEDSTOCK}$ is the mass of macroalgae biomass used in the reactor (g). W_{ASH} and $W_{MOISTURE}$ are the ash content and moisture content of the feedstock, respectively. The high heating values (HHV) of the generated bio-crude and bio-char were calculated using the proximate analysis results and the Dulong formula,[22] as follows:

$$HHV \ (MJ \ kg^{-1}) = 0.3383C + 1.422(H-O/8) \quad (2)$$

where C, H, O are the wt% present in the product. The chemical energy recovery (ER) was calculated for the bio-crude and bio-char phase according to the following equation[3]

$$ER = \left(\frac{(HHV_{PRODUCT} \times W_{PRODUCT})}{(HHV_{FEEDSTOCK} \times W_{FEEDSTOCK})} \right) \times 100 \quad (3)$$

Results and discussion

In order to obtain a more refined bio-crude from UFMA biomass, the use of UNCFO at different concentrations during the HTL process was studied. For this purpose, UNCFO was synthesized *via* the co-precipitation method. The morphology, size and phase of the products were analyzed by electron microscopy and X-ray diffraction. Fig. 1 illustrates the HRTEM images and XRD pattern of the products. The HRTEM image in Fig. 1a indicates that the products are composed of clusters containing near-spherical NPs uniformly dispersed on the Cu grid, with diameters in the range of 6–12 nm. A closer look indicates that the NPs are highly-crystalline and atomically-resolved, as seen in Fig. 1b. Extensive observations indicate that the surface of NPs is clean, smooth and without any sheathed amorphous phase, and exhibit low degree of inter-diffusion between the material itself and the surrounding medium. The diffraction peaks of the nanostructures (see Fig. 1c) were indexed to the diffraction planes of cubic inverse spinel Fe_3O_4 corresponding to the (220), (311), (400), (422), (511) and (440) planes (JCPDS # 79-0418).[23] No parasitic phases were observed indicating that the cubic Fe_3O_4 phase is of high crystalline quality and purity. The calculated lattice constant of Fe_3O_4 was $a = 0.8354 \pm 0.0003$ nm is consistent with the standard value.[17] The broadening of the diffraction peaks is ascribed to the nanocrystalline nature of the material. The calculated average crystallite size was ascertained by means of Scherrer's formula yielding ∼9 nm, or ultranano-crystalline, which is well correlated with the HRTEM analysis.

The catalytic capability and efficiency of the as-synthesized UNCFO to produce refined bio-crudes were tested *via* CHNS/O analysis. Table 1 shows the yield, higher heating values (HHV), and energy recovery (ER) of the bio-crude and bio-char after HTL processing of UFMA employing different UNCFO loadings and the reaction conditions proposed by Singh *et al.*[4] on the same biomass. These conditions are in the maximal bio-crude yield range reported by Shi *et al.*[24] Guo *et al.*[25] and many other studies.[26–32] It was found that the baseline (*i.e.*, no catalyst) bio-crude yield is 23.3 ± 0.4% for the dry biomass in ash-free basis, which was higher than the value reported (11%) by Singh and coworkers,[4] even when adjusted to our applied formula (18.78%). The increase on the yield could be due to the dichloromethane extraction in our separation process, *i.e.*, a larger range of compounds can be extracted from the liquid mixture instead of the exclusive high non polar molecules extracted with diethyl ether in their experiments. All other reaction conditions were kept constant, even the proximate
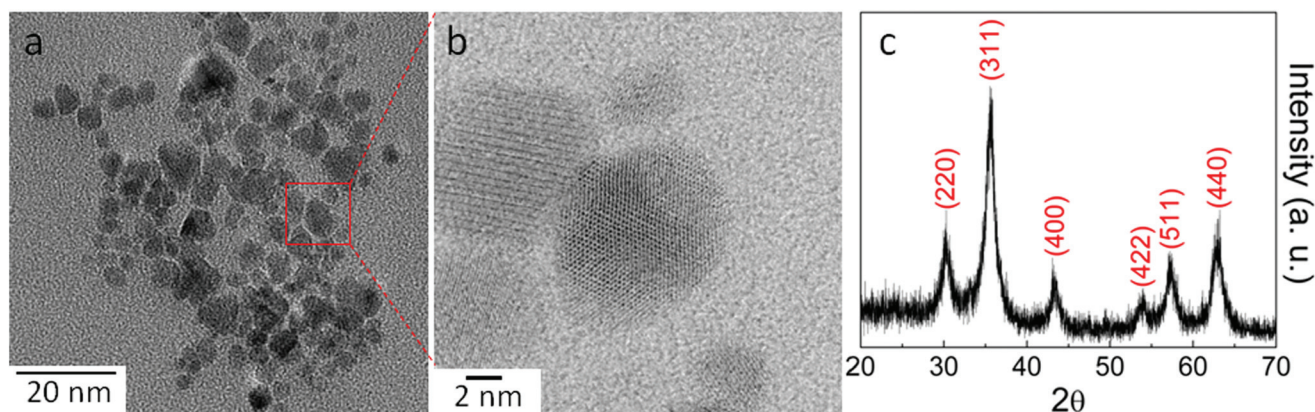
Fig. 1 (a and b) HRTEM images and (c) XRD pattern of as-synthesized UNCFO.

Table 1 Yields, HHV and ER^a for the bio-crude and bio-char obtained by HTL process employing different UNCFO loadings

UNCFOs (wt%)	Bio-crude Yield (%)	Bio-crude HHV (MJ kg^{-1})	Bio-crude ER (%)	Bio char (%)	Bio char HHV (MJ kg^{-1})	Bio-crude ER (%)	Gas yield (%)
0	23.30 ± 0.42	32.39 ± 0.24	56.52 ± 0.8	11.90 ± 0.01	30.26 ± 1.81	18.78 ± 1.03	37.06 ± 0.53
0.63	31.17 ± 0.53	29.64 ± 1.48	69.20 ± 1.2	12.52 ± 0.07	24.19 ± 0.14	28.67 ± 1.01	35.55 ± 0.22
1.25	32.36 ± 0.42	30.71 ± 0.66	74.42 ± 0.7	13.22 ± 0.02	17.62 ± 3.09	21.92 ± 0.98	32.10 ± 0.37
2.50	25.99 ± 2.11	30.80 ± 1.50	59.92 ± 1.4	13.33 ± 0.04	13.46 ± 0.10	18.02 ± 1.11	36.50 ± 0.92
3.75	25.48 ± 1.08	31.90 ± 0.56	60.87 ± 1.0	13.95 ± 0.04	11.27 ± 3.92	15.73 ± 1.12	44.91 ± 1.13

^{a} ER: energy recovery and HHV: higher heating value.

Table 2 UFMA proximate analysis

U. Fasciata proximate analysis^a

Moisture (%)	14.25 ± 0.32
Ash content (%)	10.85 ± 0.36
Protein content (%)	16.43 ± 1.21
Soluble carbohydrate content (%)	47.32 ± 3.02
Lipid content (%)	2.01 ± 0.53

^{a} Percent per dry macroalgae mass.

analysis performed over the biomass (Table 2) showed similar UFMA composition.

Likewise, an enhanced bio-crude production of 32.3 ± 0.4% (a ~9% of increase when compared to the catalyst-free yield) is obtained when 1.25 wt% of UNCFO is added. This finding is not directly comparable with the literature because there are very few studies on HTL of Ulva species and no one employed heterogeneous nanocatalyst.[3,4,33] However, it is possible to find a similar increasing trend in the Duan & Savage work for the catalytic bio-crude production of *Nannochloropsis* sp. by using bulk commercial catalysts (Pd/C, Pt/C and Ru/C).[5] The best UNCFO run shows the same proportional increase between the non-catalyzed and catalyzed reaction for noble metals. Although the metal catalyst function and catalytic mechanism are not clearly understood[24] it is necessary to

mention that the catalyst loading in the mention work was 50 wt% with respect to dry biomass, an excessive amount of catalyst when compared with our NPs loading. Jena and co-workers studied the roll of bulk NiO in the catalytic HTL of the microalgae *Spirulina platensis*[26] and it was found that the amount of oil decreased up to 24.3% when compared with non-catalytic runs while its HHV and gas production increased. Also by using Ni as a hydrothermal liquefaction catalyst, a significant increase of C in the gas phase was found. The authors argued that the Ni presence lead to tertiary reactions of organics in the bio-crude that increase the production of gases thus provoking a decrease in the bio-oil yield. All the data reported suggested that the bio-crude yield and HHV are affected by the amount and type of catalyst added.

The HHV of our bio-crude remained essentially constant between 30–32 MJ Kg^{-1}. As for the ER of the bio-crude, the highest ER value found was 74.4 ± 0.7% for a UNCFO loading of 1.25 wt%, which represents a ~18% of increase in absence of the catalyst. This observation is compatible with the corresponding increments of the yield and HHV after the HTL process. Similarly, the drop of ER values at 2.50 and 3.75 wt% correlate well with the decrease of their corresponding yields and show that the catalyst loading has a nonlinear effect on the conversion and yield. Similar behaviors have been reported in the literature for the use of iron-based catalysts in thermochemical conversion reactions.[34–36] For example, Dadyburjor and coworkers reported a nonlinear correlation between ferric

sulfide catalyst loading and the yield of oil in the coal liquefaction.[34] Bacaud and coworkers studied different iron-based catalysts for the liquefaction of coal and reported that optimal results are obtained at low ratios of catalyst/coal 0.2 to 2% iron oxide and red mud.[36] The nonlinear correlation between the loading of the catalyst and the bio-crude yield, may be attributed to different factors or a combination of them: (i) at higher loading of the catalyst, the probability of particle agglomeration increases, thus reducing the surface-to-volume ratio for interaction with the catalyst; (ii) the catalyst enhances hydrogenation, but at higher loadings H_2 is mainly consumed in the production of gases, as shown in Table 1; (iii) another possibility is that the catalyst may mediate retrograde reactions in which some products combine to produce heavier compounds that are not recovered in the bio-crude phase. Table 1 summarizes the detailed list of the values obtained for the yield, HHV and ER of the bio-char and bio-crude of marine UFMA. Taken altogether, it is clear that the HTL process is sensitive to the catalyst loading, reaching the highest value at 1.25 wt%, and that the catalyst substantially influences the chemical nature of the resultant bio-crude. In order to shed more light upon the chemical compositions of the bio-crudes, we employed FTIR spectroscopy.

The FTIR spectra of the bio-crude at different UNCFO loadings are presented in Fig. 2a, wherein the FTIR spectrum of the raw algae was included for comparison. As a whole, the spectra exhibit similar vibrational modes in the presence of the catalyst. The bands peaking at 723, 744 and 883 cm^{-1} indicate the presence of aromatic compounds. The vibrations observed can be classified, as follows: (i) the O–H bending characteristic of phenols, esters and ethers centered at 1039 cm^{-1}, (ii) the C–O stretching characteristic of alcohols peaking at 1145 and 1288 cm^{-1}; (iii) the C–H bending characteristic of fats at 1380 and 1458 cm^{-1}, (iv) the C=C stretching characteristic of alkenes centered at 1612 cm^{-1}, (v) the C=O stretching characteristic of carboxylic acids, ketones and aldehydes detected at 1672 and 1697 cm^{-1}, (vi) the C–H stretching characteristic of alkyl groups peaking at 2869, 2927 and

2933 cm^{-1}, and (vii) the water traces centered at 3350 cm^{-1}. The difference in intensity of the bands was attributed to the relative degree of abundance of certain compounds. Although the diversity of the functional groups present in the bio-crudes is apparently complex, the catalytic effect of UNCFO on the bio-crudes is marked in terms of the amount of fixed carbons that can be generated in the solid residues. Similar FTIR profiles were previously reported by other research groups working with *Ulva prolifera via* microwave-assisted direct liquefaction, and with marine brown alga *via* HTL.[21,33] No traces of iron species were detected in the bio-crudes at all UNCFO loadings, as expected. To further corroborated this observation, we conducted vibrating sample magnetometry given that UNCFO is magnetized when an external magnetic field is applied. The magnetic hysteresis loops of pristine UNCFO and of a representative bio-crude are displayed in Fig. 2b. It was observed that the pristine UNCFO reaches the magnetization saturation at ~15 kOe, and shows a coercive field (H_C) of 16.1 Oe with a near-zero remnant field, indicating a well-defined superparamagnetic behavior.[23] No magnetic response was observed in the bio-crude, confirming the absence of iron species therein.

As described above, the bio-crudes generated from the HTL process of UFMA in the presence and absence of the nanocatalyst are complex mixtures composed of more than 100 compounds; thus their identification is somewhat cumbersome. In order to obtain a more detailed characterization of the compounds, we conducted GCMS analysis. The chromatograms were analyzed using the NIST library and only compounds having a quality identification factor higher than 70 are reported. Fig. 3 shows: (a) the distribution of bio-crude compounds categorized by their energy related functionalities, (b) the most abundant fatty acids, and (c) the most abundant nitrogen containing species. It was observed that the bio-crudes are mainly composed of fatty acids, esters, alcohols, nitrogen containing heterocyclic species, hydrocarbons, aldehydes, phenols, benzene derivatives, aminoacids, aromatic compounds and ketones. The detection of these compounds is consistent with the FTIR analysis. We have identified five main
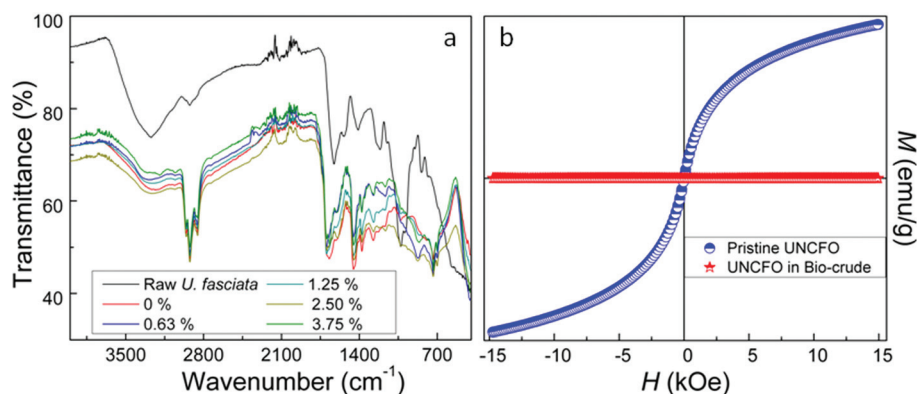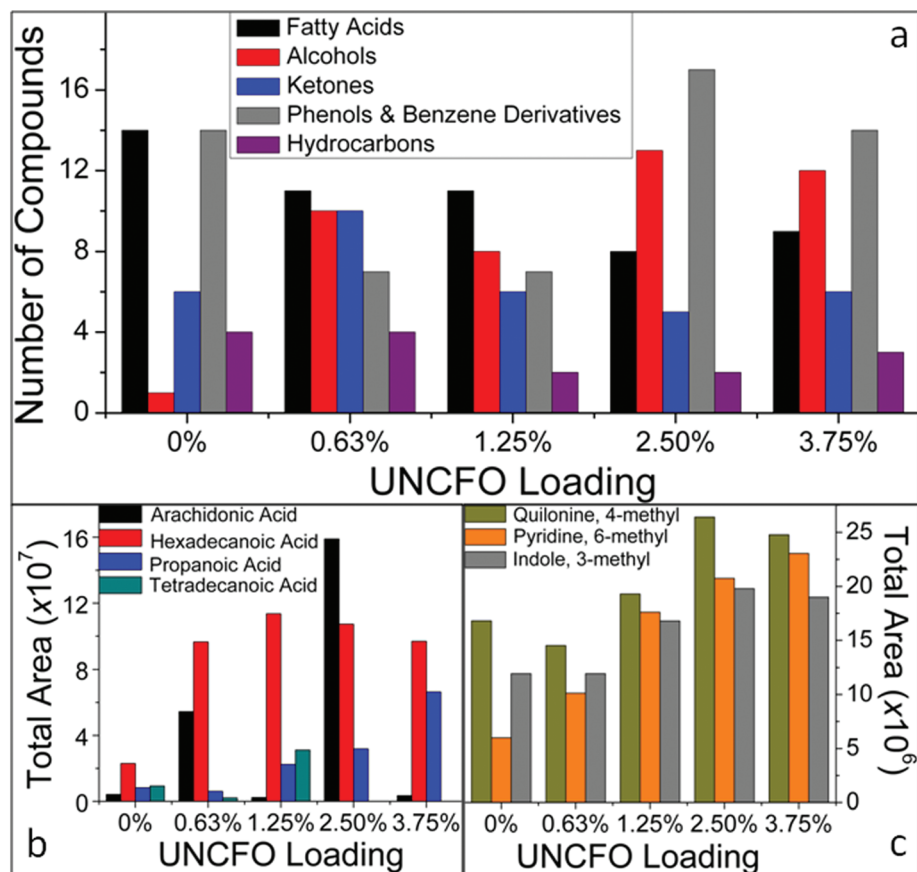

Fig. 2 (a) FTIR spectra of raw UFMA and bio-crudes produced using different UNCFO loadings, and (b) *M−H* hysteresis curves of pristine UNCFO and a representative bio-crude.

Fig. 3 Distribution of bio-crude compounds categorized by their (a) energy related functionalities, and content of (b) common fatty acids present in algae and (c) nitrogen containing species.

groups of compounds (fatty acids, alcohols, ketones, phenols and benzene derivatives, and hydrocarbons) with highly energetic functionalities in the bio-crudes, as shown in Fig. 3a. It was also found that the nitrogen containing heterocyclic compounds experience the most prominent change. In general, the variety and concentration of this type of compounds increased as the amount of catalyst increased from 0.63 to 2.50 wt% (see Fig. 3c). The presence of nitrogenated compounds (including the aromatic heterocyclic organic compound, indole) is associated to the decomposition of algal proteins. In parallel, a higher abundance of pyrazine, pyridines and other related derivatives in the presence of the catalyst was also identified, which is ascribed to the reactions between algal reducing sugars and amino acids (Maillard's reaction).[37] This is indicative of UNCFO's strong catalytic ability to favor the formation of specific products in Maillard's reactions, and is attributed to their high redox potential.[39] In terms of fatty acids, the variety of this family of compounds decreased in the presence of the catalyst (see Fig. 3a). In contrast, the abundance of propanoic acid (a short-chain fatty acid) increased in the presence of the catalyst, as seen in Fig. 3b. It was also observed that the abundance of arachidonic and tetradecanoic acids (long-chain fatty acids) do not show a well-defined tendency with respect to the UNCFO loadings, except the hexa-

decanoic acid that increases its abundance as the amount of catalyst increases. This indicates that the bio-crudes with the highest values of HHV contain higher abundances of long-chain fatty acids (C14–C20). Further observations also show the formation of additional derivatives, such as 9-methyl-tetradecanoic acid pyrrolidide, when UNCFO is used, which are associated to the condensation reaction between the fatty acids and the products obtained from the thermal decomposition of algal proteins. Their origin may be attributed to the interaction that fatty acid compounds generate with the charged surface of UNCFO, which provides an anchoring spot that catalyzes the condensation of diverse compounds with more complex structures.[38] This is supported by the fact that most metal oxides exhibit an effective influence on the chemical nature and amount of the resultant humic products (including supernatant and solid residues), which are governed by Maillard's reactions.[37] Accordingly, UNCFO substantially influences the chemical nature of the resulting bio-crudes and the amount of carbons fixed in the solid residues, in agreement with the results detailed in Table 3. Our observations also reveal that the alcohols (including butanol, hexanol and cyclohexanol) present in the bio-crudes show a tendency similar to that found for nitrogenated compounds.

Table 3 Elemental content of C, H, N, S, O and C/O ratio of the UFMA, bio-crude and bio-char at different UNCFO loadings

	UNCFO (wt%)	C (%)	H (%)	N (%)	S (%)	O^a (%)	C/O ratio
Raw *U. fasciata*	N/A	26.29 ± 2.96	4.60 ± 0.31	2.66 ± 0.13	3.13 ± 0.61	49.05 ± 3.83	0.60 ± 0.14
Bio-crude	0	70.35 ± 1.42	8.00 ± 0.35	5.81 ± 0.30	0.19 ± 0.06	15.73 ± 1.56	4.47 ± 0.07
	0.63	67.18 ± 0.66	7.43 ± 0.15	4.80 ± 0.38	N.D	20.58 ± 1.13	3.26 ± 0.05
	1.25	69.04 ± 1.04	7.56 ± 0.33	5.28 ± 0.44	N.D	19.12 ± 1.53	3.61 ± 0.08
	2.50	69.20 ± 1.48	7.44 ± 0.36	5.44 ± 0.34	N.D	17.92 ± 1.58	3.86 ± 0.09
	3.75	69.96 ± 0.43	7.78 ± 0.06	5.31 ± 0.18	N.D	15.95 ± 0.36	4.39 ± 0.02
Bio-char	0	73.69 ± 2.35	5.52 ± 0.23	4.64 ± 0.20	2.00 ± 0.32	14.15 ± 2.26	5.21 ± 0.30
	0.63	63.34 ± 2.33	4.99 ± 0.14	4.42 ± 0.12	2.88 ± 0.42	24.36 ± 2.18	2.60 ± 0.96
	1.25	52.41 ± 2.87	4.34 ± 0.25	3.75 ± 0.26	4.17 ± 0.39	35.33 ± 3.30	1.48 ± 0.11
	2.50	45.60 ± 7.5	3.97 ± 0.57	3.30 ± 0.46	4.27 ± 0.86	42.86 ± 9.18	1.06 ± 0.27
	3.75	41.90 ± 5.00	3.73 ± 0.37	2.89 ± 0.32	3.76 ± 0.21	46.15 ± 5.75	0.91 ± 0.17

^{a} Obtained by difference, N/A: not applicable, N.D: below detection limits or not detected.

As for the bio-char, it is know that part of the catalyst remained on it, and that the generated bio-crude is free of catalyst, but further analyses are needed to determine the amount of catalyst that remains in the aqueous and solid phases. As detailed in Tables 1 & 3, the production of bio-char was slightly increased from 11.9 ± 0.0% (0 wt% of UNCFO) to 13.9 ± 0.0% (3.75% of UNCFO), whereas the amount of carbons fixed in the solid residues decreased from 73.6 ± 2.3% to 41.9 ± 5.0%, respectively. This signifies that the decrease of the carbon percentage in the bio-char is related to the increase in the carbon content in the bio-crude. The bio-char also exhibits a more aromatic nature and a low fixed carbon value by increasing the loading of UNCFO. Analogously, the slight decrease (~5%) in the oxygen percentage of the bio-crude is associated to the reduction of polyketones and ketones. Similar findings were reported by Jena *et al.* working with a heterogeneous NiO catalyst *via* HTL process of *S. platensis*.[26] Compared to the bio-crude produced using homogeneous catalysts, they found a reduction of 6% in the oxygen content. The removal of UNCFO from the bio-char to further exploit its superior catalytic properties and degree of reusability will be the subject of a subsequent work, as well as the performance of the UNCFO-free as-generated bio-char as a potential fertilizer.

Conclusions

The effect of four different loadings of UNCFO on the HTL conversion of UFMA into bio-crude was comprehensively studied. We observed a significant increase of the bio-crude yield and C/O ratios as the amount of the nanocatalyst increases, reaching a peak value of 32% at 1.25 wt%. The energy recovery of the HTL process was sensitive to the catalyst loading, with a threshold value of 1.25 wt%. The detailed molecular characterization of bio-crudes *via* the HTL process represents the first systematic study done with UNCFO. Our results indicate that the nanocatalyst substantially influences the chemical nature of the resulting bio-crudes and the amount of fixed carbon in the solid residues. The resulting bio-crudes are free of iron species, which were accumulated in the generated bio-chars. The HTL process used here to produce the bio-crudes is fast, eco-friendly, energetically efficient and cost-effective, representing a step ahead to new alternatives to fossil fuels.

Notes and references

1 S. S. Toor, L. Rosendahl and A. Rudolf, *Energy*, 2011, **36**, 2328–2342.

2 S. E. Hunter and P. E. Savage, *Chem. Eng. Sci.*, 2004, **59**, 4903–4909.

3 N. Neveux, A. K. Yuen, C. Jazrawi, M. Magnusson, B. S. Haynes, A. F. Masters, A. Montoya, N. A. Paul, T. Maschmeyer and R. De Nys, *Bioresour. Technol.*, 2014, **155**, 334–341.

4 R. Singh, T. Bhaskar and B. Balagurumurthy, *Process Saf. Environ. Prot.*, 2015, **93**, 154–160.

5 P. Duan and P. E. Savage, *Ind. Eng. Chem. Res.*, 2010, **50**, 52–61.

6 J. Guo, Y. Zhuang, L. Chen, J. Liu, D. Li and N. Ye, *Bioresour. Technol.*, 2012, **120**, 19–25.

7 S. L. Holdt and S. Kraan, *J. Appl. Phycol.*, 2011, **23**, 543–597.

8 L. M. Díaz-Vázquez, A. Rojas-Pérez, M. Fuentes-Caraballo, I. V. Robles, U. Jena and K. C. Das, *Front. Energy Res.*, 2015, **3**, 1–11.

9 L. Yang, Y. Li and E. Savage, *Ind. Eng. Chem. Res.*, 2014, **53**, 1939–11944.

10 D. Zhou, L. Zhang, S. Zhang, H. Fu and J. Chen, *Energy Fuels*, 2010, **24**, 4054–4061.

11 S. Laurent, D. Forge, M. Port, A. Roch, C. Robic, L. V. Elst and R. N. Muller, *Chem. Rev.*, 2008, **108**, 2064–2110.

12 M. Akia, F. Yazdani, E. Motaee, D. Han and H. Arandiyan, *Chem. Mater.*, 2014, **1**, 16–25.

13 M. Cano, K. Sbargoud, E. Allard and C. Larpent, *Green Chem.*, 2012, **14**, 1786–1795.

14 M. Ying and G. Chen, *Appl. Biochem. Biotechnol.*, 2007, **137**, 793–803.

15 W. Xie and N. Ma, *Energy Fuels*, 2009, **23**, 1347–1353.

16 S. Hu, Y. Guan, Y. Wang and H. Han, *Appl. Energy*, 2011, **88**, 2685–2690.

17 J. Beltran-Huarac, M. J.-F. Guinel, B. R. Weiner and G. Morell, *Mater. Lett.*, 2013, **98**, 108–111.

18 J. Hedge and B. Hofreiter, *Methods Carbohydr. Chem.*, 1962, **1**, 389–390.

19 K. J. Wiechelman, R. D. Braun and J. D. Fitzpatrick, *Anal. Biochem.*, 1988, **175**, 231–237.

20 E. G. Bligh and W. J. Dyer, *Can. J. Biochem. Physiol.*, 1959, **37**, 911–917.

21 D. Li, L. Chen, D. Xu, X. Zhang, N. Ye, F. Chen and S. Chen, *Bioresour. Technol.*, 2012, **104**, 737–742.

22 Y. Qu, X. Wei and C. Zhong, *Energy*, 2003, **28**(7), 597–606.

23 J. Beltran-Huarac, S. P. Singh, M. S. Tomar, S. Pena, L. Rivera and O. J. Perales-Perez, *Mater. Res. Soc. Symp. Proc.*, 2010, **1257**, 6.

24 F. Shi, P. Wang, Y. Duan, D. Link and B. Morreale, *RSC Adv.*, 2012, **2**, 9727–9747.

25 Y. Guo, T. Yeh, W. Song, D. Xu and S. Wang, *Renewable Sustainable Energy Rev.*, 2015, **48**, 776–790.

26 U. Jena, K. C. Das and J. R. Kastner, *Appl. Energy*, 2012, **98**, 368–375.

27 S. Zou, Y. Wu, M. Yang, C. Li and J. Tong, *Energy Environ. Sci.*, 2010, **3**, 1073–1078.

28 T. M. Brown, P. Duan and P. E. Savage, *Energy Fuels*, 2010, **24**, 3639–3646.

29 K. Anastasakis and A. B. Ross, *Bioresour. Technol.*, 2011, **102**, 4876–4883.

30 Z. Shuping, W. Yulong, Y. Mingd, I. Kaleem, L. Chun and J. Tong, *Energy*, 2010, **35**, 5406–5411.

31 P. J. Valdez, M. C. Nelson, H. Y. Wang, X. N. Lin and P. E. Savage, *Biomass Bioenergy*, 2012, **46**, 317–331.

32 S. Zou, Y. Wu, M. Yang, C. Li and J. Tong, *Energy Fuels*, 2009, **23**, 3753–3758.

33 Y. Zhuang, J. Guo, L. Chen, D. Li, J. Liu and N. Ye, *Bioresour. Technol.*, 2012, **116**, 133–139.

34 D. B. Dadyburjor, W. Stewart, A. Stiller, C. Stinespring, J. Wann and J. Zondlo, *Energy Fuels*, 1994, **8**(1), 19–24.

35 J. G. Darab, J. C. Linehan and D. W. Matson, *Energy Fuels*, 1994, **8**(4), 1004–1005.

36 R. Bacaud, M. Besson and G. Djega-Mariadassou, Preprints of the American Chemical Society, Division of Fuel Chemistry, 1993, 01-juil.

37 A. Kruse, P. Maniam and F. Spieler, *Ind. Eng. Chem. Res.*, 2007, **46**(1), 87–96.

38 A. Hardie, J. Dynes, L. Kozaka and P. Huang, *Molecular Environmental Soil Science at the Interfaces in the Earth's Critical Zone*, 2010, pp. 26–28.

39 B. Thamdrup, *Adv. Microb. Ecol.*, 2000, **16**, 41–84.